Structural Engineering and Mechanics, Vol. 37, No. 4 (2011) 443-458
DOI: http://dx.doi.org/10.12989/sem.2011.37.4.443

Numerical investigation of an MR damper-based smart passive control system for mitigating vibration of stay cables

In-Ho Kim[1], Hyung-Jo Jung*[1] and Jeong-Tae Kim[2]

[1]*Department of Civil and Environmental Engineering, KAIST, Daejeon 305-701, Korea*
[2]*Department of Ocean Engineering, Pukyong National University, Busan 608-739, Korea*

(Received April 23, 2010, Accepted January 3, 2011)

Abstract. An extensive numerical investigation on the magnetorheological (MR) damper-based smart passive control system for mitigating vibration of stay cables under wind loads has been conducted. The smart passive system is incorporated with an electromagnetic induction (EMI) device for reducing complexity of the conventional MR damper based semi-active control system by eliminating an external power supply part and a feedback control part (i.e., sensors and controller). In this study, the control performance of the smart passive system has been evaluated by using a cable structure model extracted from a full-scale long stay cable with high tension. Numerical simulation results of the proposed smart damping system are compared with those of the passive and semi-active control systems employing MR dampers. It is demonstrated from the results that the control performance of the smart passive control system is better than those of the passive control cases and comparable to those of the semi-active control systems in the forced vibration analysis as well as the free vibration analysis, even though there is no external power source in the smart passive system.

Keywords: cable vibration; smart passive control system; MR damper; electromagnetic induction.

1. Introduction

Cable-stayed bridges are one of the typical civil infrastructure systems which are valuable national assets. They should be maintained to ensure economic prosperity and public safety. However, cable-stayed bridges have frequently exhibited large-amplitude vibrations of stay cables because of their large flexibility, relatively small mass and extremely low inherent damping. Since stay cables are the primary structural members in a cable-stayed bridge, these excessive vibrations of cables may cause severe structural safety and serviceability issues. In other words, they potentially induce fatigue in the cables and cable anchorages, resulting in reduction of the cable and connection life along with the risk of losing public confidence in such structures (Yamaguchi and Fujino 1998, Watson and Stafford 1998, Hikami and Shiraishi 1988).

Several methods, such as adding crossing ties or spacers, aerodynamic treatments and external passive/active dampers, have been developed to alleviate vibrations of stay cables and some of them

*Corresponding author, Associate Professor, E-mail: hjung@kaist.ac.kr

have been implemented to real scale structures, even though each has its own limitations (Yamaguchi and Fujino 1998, Johnson *et al.* 1999, 2000, 2003). Especially, discrete passive viscous dampers attached perpendicularly to the cables have been used on many bridges (e.g., Brotonne Bridge in France, Sunshine Skyway Bridge in USA, and Aratsu Bridge in Japan). Lots of investigations have been conducted to achieve the maximum damping ratio for the cable-damper systems in the case of the passive viscous dampers. Fujino and his colleagues (Sulekh 1990, Pacheco *et al*. 1993) proposed an approximate relationship between a cable configuration and the optimal damper design at a given attachment location of a damper. However, the effectiveness of a passive damper is highly dependent on its location. The performance of a damper located near the cable anchorage gets significantly worse, even though it is optimally designed. In the case of a long-span cable, therefore, a passive device can only add a small amount of damping to the cable, when it is attached at a reasonable distance (usually within 1% of the length of the cable) from the cable anchorage. On the other hand, an active transverse control method for mitigating the cable vibration has not been implemented in spite of its prominent performance, because it requires significant power sources beyond practical limits for the given number of cables and the isolated locations where controllers are placed (Yamaguchi and Dung 1992, Fujino *et al*. 1993).

In the last decade, many studies have been carried out on the semi-active control system based on a magnetorheological (MR) damper to suppress cable vibrations (Johnson *et al*. 2000, 2003, Christenson 2001, Ni and Ko 2002, Jung *et al*. 2008). However, the semi-active system requires a feedback control part (i.e., sensors, a controller and an external power source), resulting in implementation and maintenance issues for the large-scale structures. To resolve the above problems, the MR damper-based smart passive control system equipped with an electromagnetic induction (EMI) device has been recently proposed by Cho *et al*. (2005). The EMI device consists of permanent magnets and coils. Also, it converts vibratory energy of a structure into the electric energy in order to use it as the input current of the MR damper so that the vibration of the structure can be mitigated.

In this paper, the effectiveness of the smart passive control system employing an MR damper with an EMI device in mitigating cable responses is numerically investigated. In numerical simulations, a cable model extracted from a real-scale long steel stay cable with high tension, which has been installed on an in-service cable-stayed bridge in Korea, is considered. Also, by comparing its controlled responses with those of the several semi-active cases and the passive cases, the performance of the proposed system is verified.

2. Smart passive control system for cable vibration mitigation

The smart passive control system recently developed by Cho *et al*. (2005) can simplify the conventional semi-active control system based on MR dampers by replacing the feedback control part and the power supply part with the EMI device. The EMI device converts the kinetic energy of a structure to the electric energy proportional to the relative velocity between the permanent magnets and coils. Fig. 1 shows the working principle of the smart passive control system. In this figure, the solenoid coil of EMI device connected to the piston rod of the MR damper moves across the stationary magnetic field generated by permanent magnets produces induced electromotive force (*emf*) or induced current. This induced current is then used as an input to the MR damper, generating magnetic fields to change the damping characteristics of the damper. Therefore, the smart

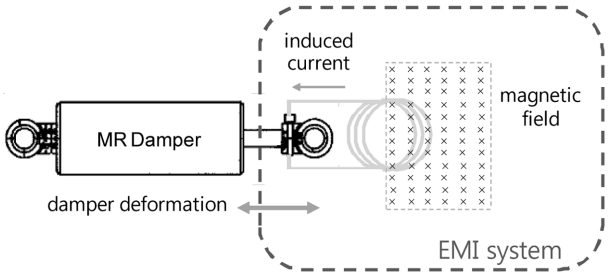

Fig. 1 Smart passive system consisting of an MR damper and an EMI device

passive control device does not need any external power at all.

According to the Faraday's law of electromagnetic induction, the induced *emf* can be calculated as

$$\varepsilon = -n\frac{d\phi_b}{dt} = -nB\frac{dA}{dt} \tag{1}$$

where ε denotes the induced *emf* with the unit of volts (V), n is the number of turns of coils, ϕ_b is the magnetic flux, B is the force of magnetic field and A is the area of the cross section of magnetic field. Eq. (1) means that the induced *emf* in a closed loop is equal to the negative of the time rate of a change in the magnet flux through the loop. As seen from the equation, the amount of the induced *emf* can be controlled by the turns of the coil (n) or the intensity of the permanent magnet (B).

3. Numerical simulation

3.1 Cable model

For numerical simulations, a simple taut cable-damper system is considered as shown in Fig. 2. It is assumed that a cable model has small sag (within 0.1% sag-to-length ratio) so that the motion of the cable can be modeled by the motion of a taut string (Irvine 1981). Then, the transverse motion of the cable with a damper in a linear range is expressed as

$$m\ddot{v}(x,t) + c\dot{v}(x,t) - Tv''(x,t) = F_w(x,t) + F_d(t)\delta(x - x_d) \tag{2}$$

where $v(x,t)$ is the transverse deflection of the cable, m is the cable mass per unit length, c is the viscous damping per unit length, x_d is the damper location, $F_w(x,t)$ is external wind load, $F_d(t)$ is the MR damper force and $\delta(\cdot)$ is the Dirac delta function.

It is assumed that the transverse deflection may be approximated using a finite series

$$v(x,t) = \sum_{j=1}^{n} q_j(t)\phi_j(x) \tag{3}$$

where n is the number of modes considered, $q_j(t)$ is the generalized displacements and $\phi_j(x)$ is a set of shape functions (the geometric boundary conditions $\phi_j(0) = \phi_j(1) = 0$).

According to Johnson *et al*. (2000), introducing shape functions based on the deflection due to a

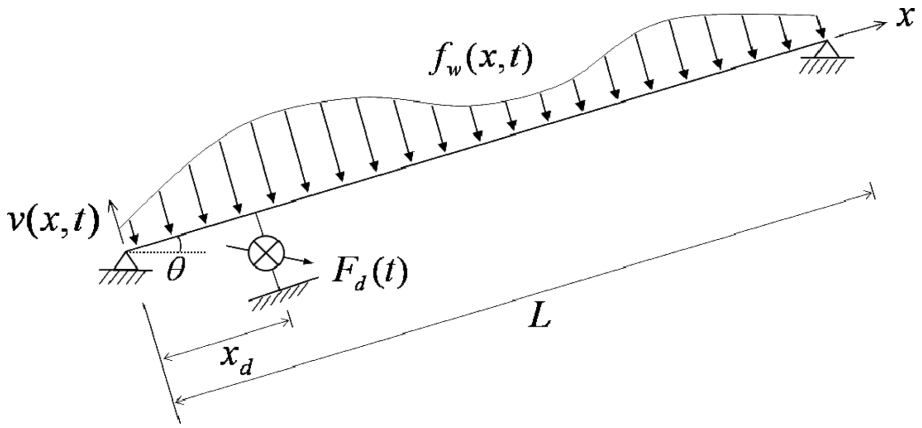

Fig. 2 Taut cable-damper system

static force at the damper (see Eqs. (4a)) can reduce the number of terms required for comparable accuracy; on the other hand, hundreds of terms in the sine series are generally used as shape functions if this static deflection is not considered, resulting in considerable computation effort.

$$\phi_1(x) = \begin{cases} x/x_d & 0 \le x \le x_d \\ (L-x)/(L-x_d) & x_d \le x \le L \end{cases} \tag{4a}$$

$$\phi_{j+1}(x) = \sin \pi j\left(\frac{x}{L}\right) \qquad j = 1, 2, \ldots, n-2 \tag{4b}$$

The non-dimensional equation of motion written in matrix form from a standard Galerkin method can be expressed as follows (Craig 1981)

$$M\ddot{q}(t) + C\dot{q}(t) + Kq(t) = F_w(x,t) + \varphi_d F_d(t) \tag{5}$$

or

$$[m\int_0^L \phi_i(x)\phi_j(x)dx]\ddot{q}(t) + [c\int_0^L \phi_i(x)\phi_j(x)dx]\dot{q}(t) + [-T\int_0^L \phi_i'(x)\phi_j'(x)dx]q(t) = \int_0^L f(x,t)\phi_i(x)dx + \varphi_d F_d(t) \tag{6}$$

where M is the mass matrix, C is the damping matrix (the evaluated damping matrix associated with the given set of modal damping ratios), K is the stiffness matrix and the damper vectors φ_d

$$\varphi_d = \phi(x_d) = [\phi_1(x_d) \;\; \phi_2(x_d) \;\; \ldots \;\; \phi_n(x_d)]^T \tag{7}$$

This equation can be written in state-space form as

$$\begin{Bmatrix} \dot{q} \\ \ddot{q} \end{Bmatrix} = \begin{bmatrix} 0 & I \\ -M^{-1}K & -M^{-1}C \end{bmatrix} \begin{Bmatrix} q \\ \dot{q} \end{Bmatrix} + \begin{bmatrix} 0 \\ M^{-1}\varphi_d \end{bmatrix} F_d + \begin{bmatrix} 0 \\ M^{-1} \end{bmatrix} f \tag{8}$$

Table 1 Cable characteristics

Parameter	Value
Length (l)	203.2 m
Mass per unit length (m)	51.3 kg/m
Tension (T)	2659.21 kN
Diameter	115 mm

$$\begin{Bmatrix} q \\ \dot{q} \\ \ddot{q} \end{Bmatrix} = \begin{bmatrix} I & 0 \\ 0 & I \\ -M^{-1}K & -M^{-1}C \end{bmatrix} \begin{Bmatrix} q \\ \dot{q} \end{Bmatrix} + \begin{bmatrix} 0 \\ 0 \\ M^{-1}\varphi_d \end{bmatrix} F_d + \begin{bmatrix} 0 \\ 0 \\ M^{-1} \end{bmatrix} f + n \tag{9}$$

$$y = \begin{bmatrix} \varphi_d^T & 0 \\ -\varphi_d^T M^{-1}K & -\varphi_d^T M^{-1}C \end{bmatrix} \begin{Bmatrix} q \\ \dot{q} \end{Bmatrix} + \begin{bmatrix} 0 \\ \varphi_d^T M^{-1}\varphi_d \end{bmatrix} F_d + \begin{bmatrix} 0 \\ \varphi_d^T M^{-1} \end{bmatrix} f + n \tag{10}$$

where $y = [v(x_d, t) \;\; \ddot{v}(x_d, t)] + n$ is a vector of noisy sensor measurements, and n is a vector of stochastic sensor noise processes.

To numerically evaluate the control performance of smart passive control system, the cable model is extracted from a 203.2 m long steel high-tension stay cable used in an actual cable-stayed bridge. The material properties of the cable are presented in Table 1.

3.2 Magnetorheological (MR) dampers

The semi-active devices such as MR damper are distinguished from active control devices in the fact that they can produce only dissipative force and different from passive control devices in the fact that characteristics of devices can be changed in real time. Therefore, variable MR damper model was developed by many researchers. In this study, the parameters of the MR damper identified by Terasawa *et al*. (2004) are used after adjusting them by magnification factors. At the dynamic model of an MR damper, damper force $F_d(t)$ is expressed by

$$F_d = \sigma_a \eta + \sigma_0 \eta u + \sigma_1 \dot{\eta} + \sigma_2 \dot{x} + \sigma_b \dot{x} u \tag{11}$$

$$\dot{\eta} = \dot{x} - a_0 |\dot{x}| \eta \tag{12}$$

where the variables and each parameters are defined as:

$\eta(t)$: Internal state variable (m)

$\dot{x}(t)$: Velocity of the cable where MR damper is attached (m/s)

σ_0: Stiffness of $\eta(t)$ influenced by $u(t)$ (N/(m·V))

σ_1: Damping coefficient of $\eta(t)$ (N·s/m)

σ_2: Viscous damping coefficient (N·s/m)

σ_a: Stiffness of $\eta(t)$ (N/m)

σ_b: Viscous damping coefficient influenced by $u(t)$ (N·s/(m·V))

a_0: Constant value (1/m)

$u(t)$: Input voltage of MR damper (V)

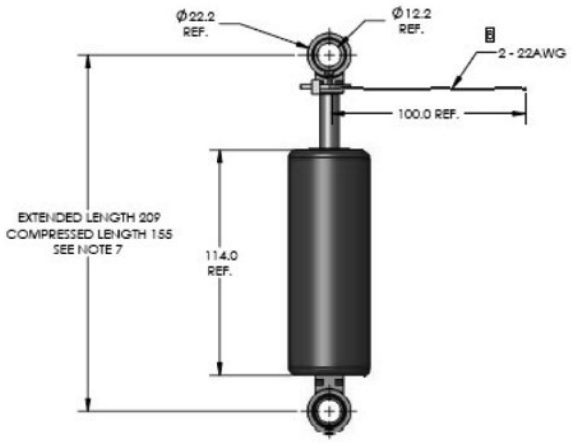

Fig. 3 MR damper (RD-1005-03, Load Corp.)

Table 2 Parameters for damper model (MF = 20)

Parameter	Value	Parameter	Value
σ_0 (N/(mV))	28815 MF	σ_a (N/m)	30542 MF
σ_1 (Ns/m)	0.131 MF	σ_b (N/(mV))	16.3 MF
σ_2 (Ns/m)	29.6 MF	σ_2 (Ns/m)	3198 MF

A schematic of the MR damper used in the numerical simulation is shown in Fig. 3. Table 2 shows the parameters of MR damper proposed by Terasawa *et al*. (2004). The damper is attached transversely to the cable at the location of 6.096 m (3% of the cable length) from the bottom supports and the damper setup with EMI system can provide in-plane forces transverse to the cable. The maximum capacity of the damper is assumed to be about 2,000 N.

3.3 Comparison of control methods

In this study, the control performance of the proposed smart passive system is verified by comparing with the passive control cases based on MR dampers and three semi-active control algorithms (i.e., the modulated homogeneous friction algorithm, Control based on Lyapunov stability theory, and maximum energy dissipation algorithm (Choi *et al*. 2008)). For the passive cases, an MR damper is operated with the different constant voltage inputs from 0 Volt to 4.45 Volt. For the semi-active control cases, each algorithm is partially modified for application to the cable-damper system. The basic principle of each algorithm is briefly introduced at this section and more detailed information of each algorithm can be found in Jansen and Dyke (2000). Table 3 shows all the control methods considered in this study. As shown in the table, the proposed smart passive system can be considered as one of the passive control methods because it does not need the external power.

Table 3 Comparison of control methods

Control method	Control type
Passive-off (input voltage = 0 V) Passive-on (input voltage = 4.45 V)	Passive control
Lyapunov stability theory based control (Lyapunov) Maximum energy dissipation (MED) Modulated homogeneous friction (MHF)	Semi-active control
Smart passive control	Passive control

3.3.1 Control algorithm based on Lyapunov stability theory

The state is stable in the sense of Lyapunov when the rate of change of the Lyapunov function is negative semi-definite, according to the Lyapunov stability theory. Leitmann (1994) applied Lyapunov's direct approach to design a semi-active controller. In the approach, the goal of the control law is to choose control inputs that will result in making the following rate of change of the Lyapunov function as possible

$$\dot{V}_L = -\frac{1}{2}z^T Q_P z + z^T P_L B F_d + z^T P_L G f \tag{13}$$

where z is the state vector, and P_L is the real, symmetric, positive definite matrix satisfying the following Lyapunov equation

$$A P_L + P_L A^T = -Q_P \tag{14}$$

for a positive semi-definite matrix Q_P.

The only term in Eq. (13) which can be directly affected by a change in the control voltage is the second term in the right-hand side, which contains the force vector F_d. Thus, the control law which will minimize $\dot{V}_L$ is

$$V = V_{\max} H((-z)^T P_L B F_d) \tag{15}$$

where $V_{\max}$ is the maximum voltage input to an MR fluid damper, and $H(\cdot)$ is the heaviside step function.

3.3.2 Maximum energy dissipation algorithm

McClamroch and Gavin (1995) developed the maximum energy dissipation algorithm as a variation of the decentralized bang-bang approach. In the maximum energy dissipation algorithm, the Lyapunov function was chosen to represent the relative total vibratory energy in the system as (Jansen and Dyke 2000)

$$V_L = \frac{1}{2}\eta^T K \eta + \frac{1}{2}\dot{\eta}^T M \dot{\eta} \tag{16}$$

Calculating the rate of change of the Lyapunov function from Eq. (16), the term which can be directly affected by changes in the control voltage is identified and the control law for semi-active

controller attached to cable is obtained as

$$V = V_{\max} H(-\dot{\eta}\varphi F_d) \tag{17}$$

This control algorithm commands the maximum control voltage when the cable system dissipates energy.

3.3.3 Modulated homogeneous friction algorithm

Inaudi (1997) originally proposed the modulated homogeneous friction algorithm for the controller using a variable fiction damper. However, it can be adopted for an MR damper due to its strong similarities between the behavior of a variable friction device and the MR damper. This algorithm commands more slip force with damper deformation larger by increasing the damping coefficient to improve the energy dissipation process of semi-active dampers. In this approach, at every local extreme deformation of the device the desired control force F_{d_n} can be determined as

$$F_{d_n} = g_n[P[v_d(t)]] \tag{18}$$

where g_n is the positive gain, the operator $P[\cdot]$ is defined as

$$P[\Delta_i(t)] = \Delta_i(t-s) \tag{19}$$

for $s = \{\min x \geq 0 | \dot{\Delta}_i(t-x) = 0\}$ and $\Delta_i(t-s)$ is the most recent local extreme deformation of the device.

Because the force produced by the MR damper cannot be directly commanded, the force level, or the command voltage input to dampers, is renewed as follows

$$V = V_{\max} H(F_{d_n} - |F_d|) \tag{20}$$

3.4 Evaluation criteria

All of the control algorithms are evaluated using a set of evaluation criteria (Jung *et al*. 2008). The first and second evaluation criteria are measurements of the displacement at mid-span (J_1) and quarter-span (J_2). The third and forth evaluation criteria are root mean square (RMS) of cable deflection (J_3) and velocity (J_4) over the entire simulation time. Four evaluation criteria of responses are defined by

$$J_1 = \frac{\max(v_{midspan}(t))}{\max(v_{midspan}(t))|_{uncontrolled}} \tag{21}$$

$$J_2 = \frac{\max(v_{quarterspan}(t))}{\max(v_{quarterspan}(t))|_{uncontrolled}} \tag{22}$$

$$J_3 = \frac{\sigma^2_{displacement}}{\sigma^2_{displacement}|_{uncontrolled}} \tag{23}$$

$$J_4 = \frac{\sigma^2_{velocity}}{\sigma^2_{velocity}\big|_{uncontrolled}} \tag{24}$$

where $$\sigma^2_{displacement} = E[\int_0^L v^2(x,t)dx] = trace\{M^{1/2}E[\eta(t)\eta^T(t)]M^{1/2}\} \tag{25}$$

$$\sigma^2_{velocity} = E[\int_0^L v^2(x,t)dx] = trace\{M^{1/2}E[\dot{\eta}(t)\dot{\eta}^T(t)]M^{1/2}\} \tag{26}$$

3.5 External load

For numerical simulations, the external wind load is calculated based on the wind speed. First, the actual wind speed was directly measured on an in-service cable-stayed bridge in Korea as shown in Fig. 4. And then, the wind load can be obtained by using the following equation

$$f(t) = \frac{1}{2}\cdot\rho\cdot C\cdot A\cdot V^2\cdot sign(V) \tag{27}$$

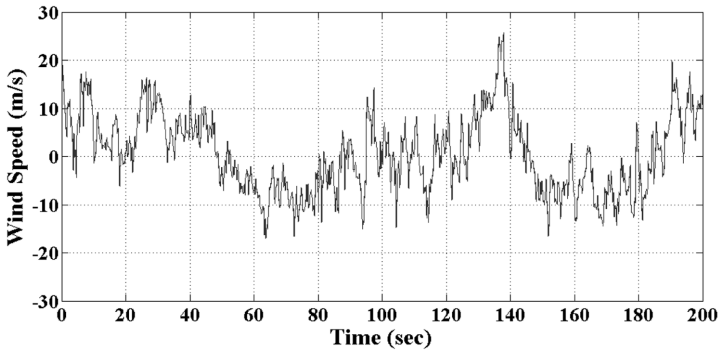

Fig. 4 The measured wind speed

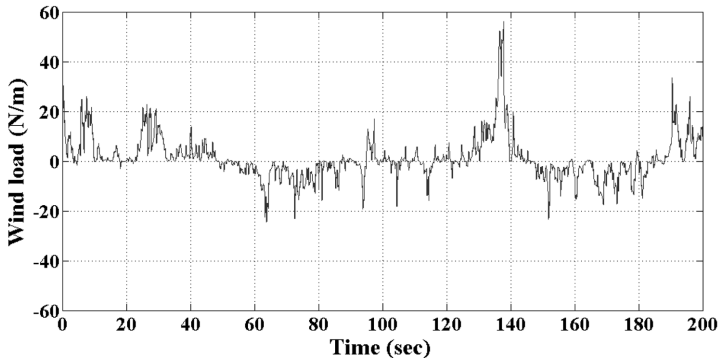

Fig. 5 The generated wind load

where ρ is the air density (1.25 N·s^2/m^4), C is the wind force coefficient (1.2), A is the area under the wind load, V is the measured wind speed. Fig. 5 shows the calculated wind load based on Fig. 4 and Eq. (27).

Numerical simulations of the two cases have been carried out. First, the forced vibration analysis using the calculated wind load based on the measured wind speed data is considered. And then, the peak response in each control case is compared. Also, the free vibration analysis is performed in order to verify the effectiveness of the proposed system through the damping ratio of the cable-damper system.

3.6 Forced vibration analysis results

Fig. 6 shows the time history responses of the displacement at the mid-point of the cable in the passive-off (i.e., the input voltage of 0 V) and passive-on (i.e., the input voltage of 4.45 V) cases under the calculated wind load. As seen from the figures, the passive-off case can slightly reduce the cable response compared to the uncontrolled case; on the other hand, the passive-on case can significantly mitigate the vibration of the cable. Fig. 7 shows the corresponding damper force of the MR damper in the passive control cases. The damper force in the passive-on case is much larger than that in the passive-off case.

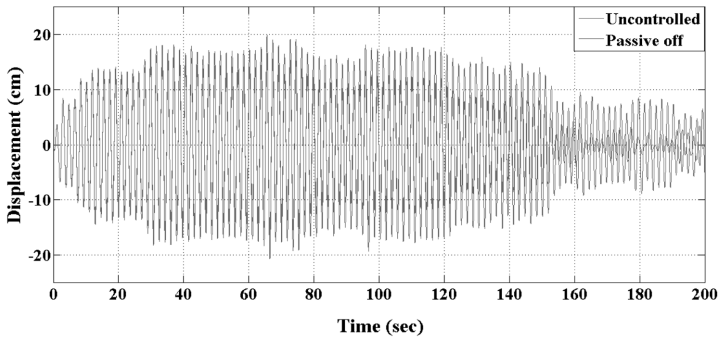

(a) Passive-off case

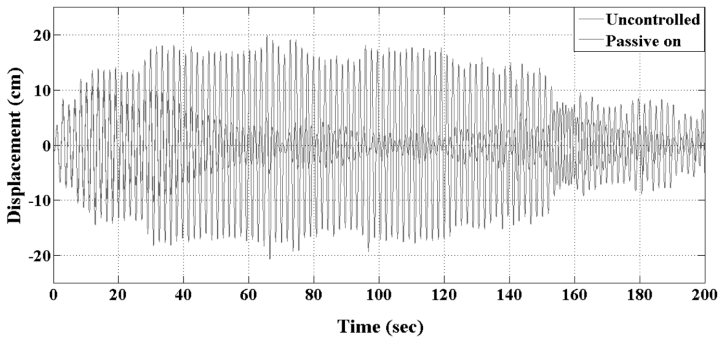

(b) Passive-on case

Fig. 6 Mid-point displacement of the passive control methods

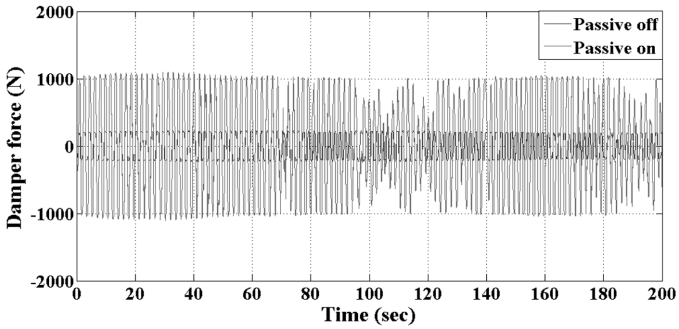

Fig. 7 Damper force of the MR damper in the passive control cases

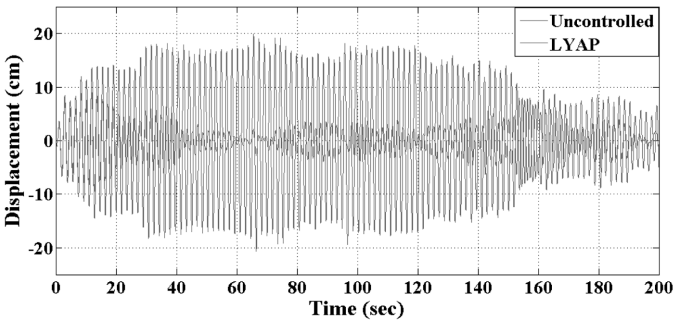

(a) Control based on Lyapunov stability theory (Lyapunov)

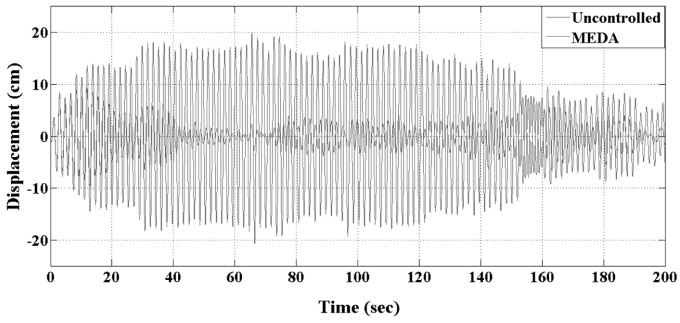

(b) Maximum energy dissipation (MED)

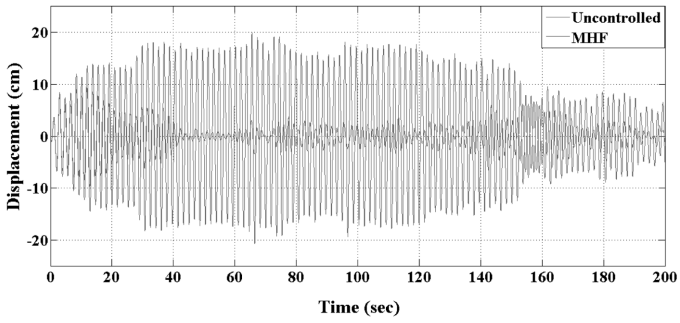

(c) Modulated homogeneous friction (MHF)

Fig. 8 Mid-point displacement of the semi-active control cases

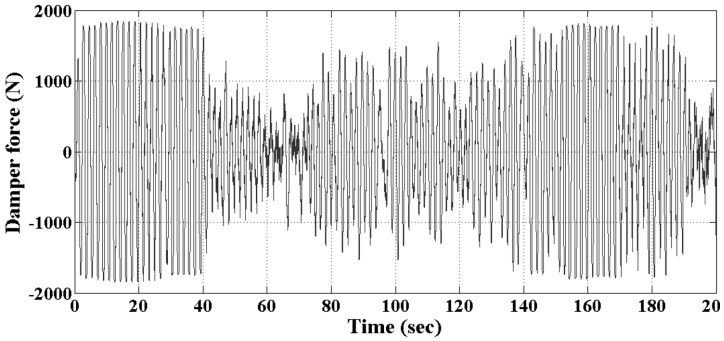

(a) Control based on Lyapunov stability theory (Lyapunov)

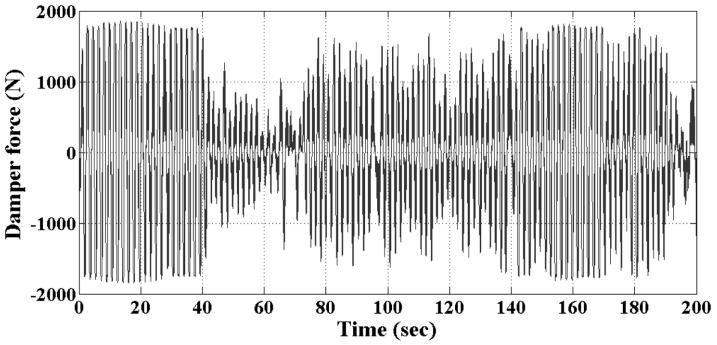

(b) Maximum energy dissipation (MED)

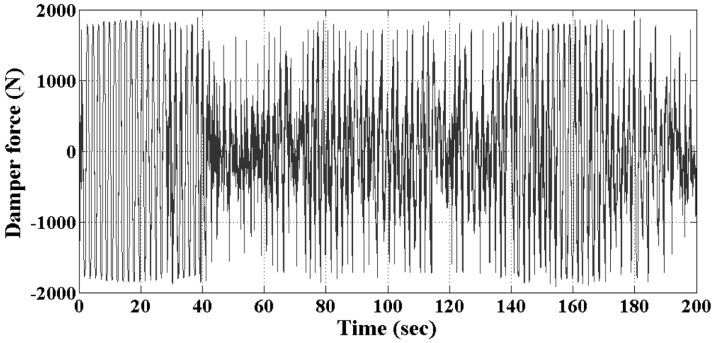

(c) Modulated homogeneous friction (MHF)

Fig. 9 Damper force of the MR damper in the semi-active control cases

The time history responses of the displacement at the mid-point of the cable in the semi-active control cases are shown in Fig. 8. These figures indicate that all the semi-active systems (i.e., control based on Lyapunov stability theory (Lyapunov), maximum energy dissipation (MED) and modulated homogeneous friction (MHF)) can significantly reduce the displacement response of the cable compared to the uncontrolled case. Fig. 9 shows the corresponding MR damper forces in all the semi-active control cases.

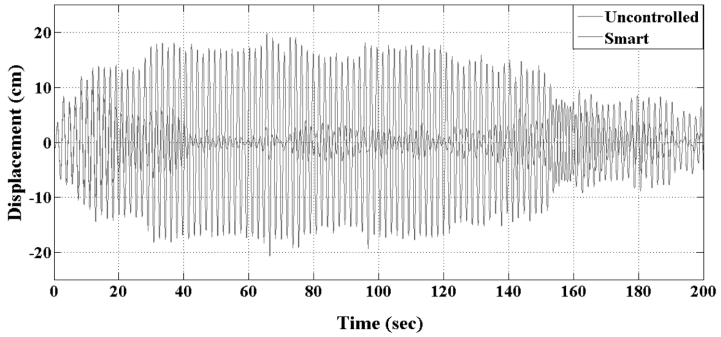

Fig. 10 Mid-point displacement of the smart passive control system

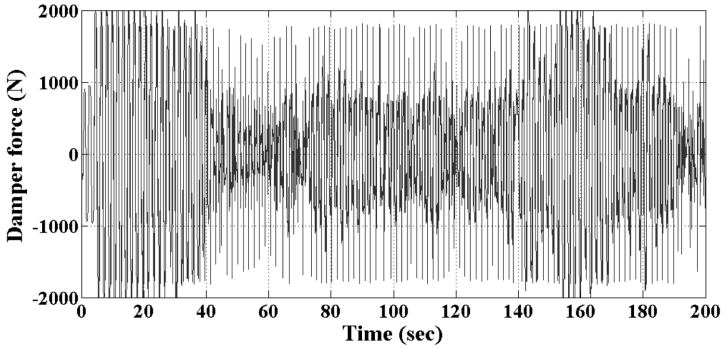

Fig. 11 Damper force of the MR damper in the smart passive control system

Fig. 10 represents the time history responses of the displacement at the mid-point of the cable in the smart passive case. As seen from the figure, the mid-point displacement in the smart passive system is dramatically reduced. Also, by comparing Figs. 6, 8 and 10, it is known that the response mitigation performance of the smart passive system is slightly better than that of the passive-on case and comparable to those of all the semi-active cases. Fig. 11 shows the corresponding MR damper force in the smart passive case.

Table 4 shows the normalized responses of control algorithms with respect to the uncontrolled system. As shown in the table, all the control algorithms, except the passive-off case, significantly reduce the responses compared with the uncontrolled system (i.e., 45~65% reduction in the passive-on case, 50~71% in Lyapunov, 51~72% in MED, 50~74% in MHF, 49~72% in the smart passive case). In the passively operated systems, the performance of the passive-on is much better than that of the passive-off system. Of all the semi-active control algorithms, the modulated homogeneous (MHF) algorithm is slightly better than the other two algorithms as well as the passive-on system.

In the table, the value in the parenthesis represents the ratio of the normalized response in each control case to that in the smart passive case. That is, if the values in a specific control system are larger than one, it means that the smart passive system has the better performance than the control system. As seen from the table, all the values in parenthesis in the passive control systems are larger than one. It clearly indicates that the smart passive system has the better performance than the passive cases. On the other hand, one of the semi-active cases such as MHF shows a little bit better

Table 4 Normalized responses with respect to the uncontrolled system

Control algorithms	Passive off	Passive on	Lyapunov	MED	MHF	Smart passive
J_1 (max. displ. at mid-point)	0.84 (1.79)	0.55 (1.17)	0.46 (0.98)	0.45 (0.96)	0.46 (0.98)	0.47 (1.0)
J_2 (max. displ. at quarter-point)	0.79 (1.55)	0.54 (1.1)	0.50 (0.98)	0.49 (0.96)	0.50 (0.98)	0.51 (1.0)
J_3 (RMS displ.)	0.73 (2.61)	0.35 (1.25)	0.29 (1.05)	0.28 (1.0)	0.26 (0.93)	0.28 (1.0)
J_4 (RMS velocity)	0.74 (2.64)	0.35 (1.25)	0.30 (1.07)	0.29 (1.03)	0.26 (0.93)	0.28 (1.0)

performance than the smart passive case by 2~7% and the other two semi-active cases have the similar performance to the smart passive case. Also, the proposed smart passive system has a crucial advantage such as the simplicity (i.e., no need to external power source, sensors and a controller). Therefore, it could be considered as an alternative vibration mitigation system for stay cables.

3.7 Free vibration analysis results

Because a stay cable with a damper shows nonlinear dynamic behavior, the amplitude-dependent damping ratio of the cable-damper system can be calculated by using the Hilbert transform-based identification method (Duan *et al*. 2002). Fig. 12 shows the first modal damping ratio of each control system with the variation of the vibration amplitude. According to the figure, the damping ratio of the modulated homogeneous friction algorithm has the largest value. And, the damping ratios of the other two semi-active control algorithms and the smart passive system have larger than those of the passive control methods (i.e., the passive-off and passive-on cases). Therefore, it is clearly demonstrated that the smart passive system could be one of the promising candidates for mitigating the excessive vibration of stay cables under wind load.

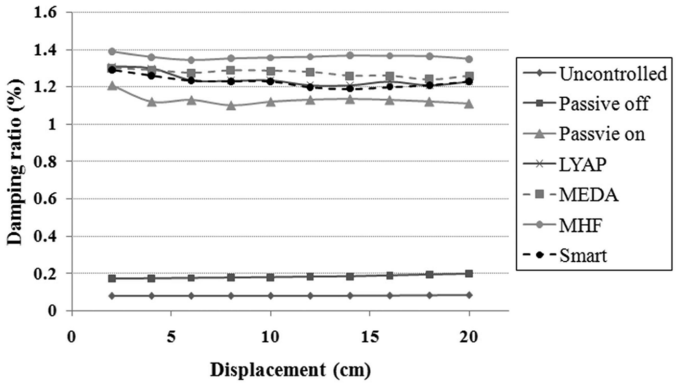

Fig. 12 Damping ratios of each control system

4. Conclusions

In this study, the smart passive control system consisting of the MR damper and the EMI device has been numerically investigated to validate its efficacy for real scaled stay cable vibration reduction. To this end, the forced and free vibration analyses have been carried out by using a cable model data extracted from a 203 m real-scaled stay cable in the in-service cable-stayed bridge in Korea. And then, numerical simulation results of the smart passive system are compared with those of passive cases (the passive-off and passive-on cases) and semi-active control systems (the modulated homogeneous friction, maximum energy dissipation and Lyapunov stability based control) employing MR dampers. As a result, the control performance of the smart passive control system is better than those of the passive control cases and comparable to those of the semi-active control systems in the forced vibration analysis as well as the free vibration analysis, even though there is no external power source in the system. Therefore, the MR damper-based smart passive control system employing an EMI device could be considered as one of the promising strategies for cable vibration mitigation. The control effectiveness of the smart passive system will be experimentally validated by using a full-scale structure.

Acknowledgements

This work was supported by the Korea Research Foundation Grant (KRF-2006-003-D00460) and the Smart Infra-Structure Technology Center (SISTeC) from the Ministry of Science and Technology in Korea. Their supports are gratefully appreciated.

References

Cho, S.W., Jung, H.J. and Lee, I.W. (2005), "Smart passive control system based on magnetorheological damper", *Smart Mater. Struct.*, **14**, 707-714.

Choi, K.M., Lee, H.J., Cho, S.W. and Lee, I.W. (2008), "Modified energy dissipation algorithm for seismic structures using magnetorheological damper", *KSCE J. Civil Eng.*, **11**, 121-126.

Christenson, R.E. (2001), "Semiactive control of civil structures for natural hazard mitigation: analytical and experimental studies", Ph.D. Dissertation, Department of Civil Engineering and Geological Sciences, University of Notre Dame, Indiana.

Craig, R., Jr. (1981), *Structural Dynamics*: *An Introduction to Computer Method*, Wiley, New York.

Deodatis, G. (1996), "Simulation of ergodic multivariate stochastic processes", *J. Eng. Mech.-ASCE*, **122**, 778-787.

Duan, Y.F., Ko, J.M., Ni, Y.Q. and Chen, Z.Q. (2002), "Field comparative tests of cable vibration control using MR dampers in single and twin damper setups", *Advances in Steel Structures,* Elsevier, Oxford.

Hikami, Y. and Shiraishi, N. (1988), "Rain-wind induced vibration of cables in cable-stayed bridges", *J. Wind Eng. Ind. Aerod.*, **29**, 409-418.

Irvine, H.M. (1981), *Cable Structures*, MIT Press, Cambridge, Massachusetts.

Jansen, L.M. and Dyke, S.J. (2000), "Semiactive control strategies for MR dampers: comparative study", *J. Eng. Mech.-ASCE*, **126**(8), 795-803.

Johnson, E.A., Spencer, B.F., Jr. and Fujino, Y. (1999), "Semiactive damping of stay cables: a preliminary study", *Proceedings of the Seventeenth International Modal Analysis Conference*, Florida, USA.

Johnson, E.A., Baker, G.A., Spencer, B.F., Jr. and Fujino, Y. (2000), "Mitigating stay cable oscillation using semiactive damping", *Smart Structures and Materials 2000: Smart Systems for Bridges, Structures, and*

Highways (Ed. Liu, S.C.), *Proceedings of SPIE*, **3988**, 207-216.
Johnson, E.A., Christenson, R.E. and Spencer, B.F., Jr. (2003), "Semiactive damping of cables with sag", *Comput-Aided Civ. Inf.,* **18**(2), 132-146.
Jung, H.J., Choi, K.M., Park, K.S. and Cho, S.W. (2007), "Seismic protection of base isolated structures using smart passive control system", *Smart Struct. Syst.*, **3**, 385-403.
Jung, H.J., Jang, J.E., Choi, K.M. and Lee, H.J. (2008), "MR fluid damper-based smart damping systems for long steel stay cable under wind load", *Smart Struct. Syst.*, **4**, 697-710.
Kaimal, J.C., Wyngaard, J.C., Izumi, Y. and Coté, O.R. (1972), "Spectral characteristics of surface-layer turbulence", *Journal Royal Meteorological Society*, **98**, 563-589.
Kim, I.H., Lee, S.W., Lee, H.J. and Jung, H.J. (2008), "Experimental validation of smart passive system for cable vibration mitigation", *Proceedings of the 21st KKCNN Symposium on Civil Engineering*, Singapore.
Ko, J.M., Chen, Z.Q., Duan, Y.F. and Ni, Y.Q. (2002), "Field vibration tests of bridge stay cables incorporated with magnetorheological dampers", *Smart Structures and Materials 2002: Smart Systems for Bridges, Structures, and Highways* (Eds. Liu, S.C. and Pines, D.J.), *Proceedings of SPIE*, **4696**, 30-40.
Ni, Y.Q., Duan, Y.F., Chen, Z.Q. and Ko, J.M. (2002), "Damping identification of MR-damped bridge cables from in-situ monitoring under wind-rain-excited conditions", *Smart Structures and Materials 2002: Smart Systems for Bridges, Structures, and Highways* (Eds. Liu, S.C. and Pines, D.J.), **4696**, 41-51.
Pacheco, B.M., Fujino, Y. and Sulekh, A. (1993), "Estimation curve for modal damping in stay cables with viscous damper", *J. Struct. Eng.-ASCE*, **119**(6), 1961-1979.
Sulekh, A. (1990), "Non-dimensionalized curves for modal damping in stay cables with viscous dampers", Master Thesis, Department of Civil Engineering, University of Tokyo, Tokyo, Japan.
Terasawa, T., Sakai, C., Ohmori, H. and Sano, A. (2004), "Adaptive identification of MR damper for vibration control", *Proceedings of the 43rd IEEE Conference on Decision and Control*, Bahamas, December.
Watson, S.C. and Stafford, D. (1988), "Cables in trouble", *Civil Eng.-ASCE*, **58**, 38-41.
Yamaguchi, H. and Dung, N.N. (1992), "Active wave control of sagged-cable vibration", *Proceedings of the First International Conference on Motion and Vibration Control*, Yokohama, Japan.
Yamaguchi, H. and Fujino, Y. (1998), "Stayed cable dynamics and its vibration control", *Proceedings of the International Symposium on Advances in Bridge Aerodynamics*, Copenhagen, Denmark.